J. Fluid Mech. (2013), *vol.* 736, *pp.* 107–129. © Cambridge University Press 2013
doi:10.1017/jfm.2013.530

Inertial instability of flows on the inside or outside of a rotating horizontal cylinder

E. S. Benilov† and V. N. Lapin

Department of Mathematics and Statistics, University of Limerick, Limerick, Ireland

(Received 30 April 2013; revised 12 August 2013; accepted 1 October 2013;
first published online 1 November 2013)

We consider thin liquid films on the inside (rimming flows) or outside (coating flows) of a cylinder with horizontal axis, rotating about this axis. If the liquid's net volume is small, such films are known to evolve towards a steady state with a smooth surface, whereas, for larger amounts, the flow develops a 'shock' similar to a tidal bore. In this work, smooth films are shown to be unstable. Since the strongest instability occurs at wavelengths comparable to the film's thickness, our analysis is based on the full Navier–Stokes equations, not on the lubrication approximation (which has been traditionally used in this problem). It is also shown that, for cylinders of sufficiently small radii, the instability can be suppressed by surface tension.

Key words: instability, interfacial flows (free surface), thin films

1. Introduction

Interest in flows on a rotating horizontal cylinder originates from a question raised by Moffatt (1977), as to how much honey one can keep on a spoon by holding it horizontally and permanently turning it. Approximating the spoon by a cylinder and assuming the layer of the liquid (honey) to be thin, Moffatt (1977) found a family of solutions describing steady flows around the cylinder. These solutions can be ordered in accordance with their 'loads' (i.e. the liquid's net volume), with the maximum load corresponding to a certain limiting solution – which seemed to provide a qualitative answer to the question of how much honey one can keep on a rotating spoon.

Note that Moffatt's (1977) results are applicable to both *coating* and *rimming* flows, i.e. on the *outside* and *inside* of a rotating horizontal cylinder. The similarity of the two problems stems from the fact that the depth of the liquid layer in both cases is usually assumed to be much smaller than the cylinder's radius, so the geometry of the flow is, to leading order, Cartesian. Thus, in what follows, when describing results that are valid for both problems, we shall not mention for which one they were obtained originally.

It turned out, however, that other solutions exist for coating and rimming flows. Firstly, Benjamin, Pritchard & Tavener (1993) and O'Brien & Gath (1998) found flows with a shock similar to a tidal bore, with loads exceeding those of Moffatt's (1977) smooth solutions. Secondly, Ashmore, Hosoi & Stone (2003) and Benilov, Benilov & Kopteva (2008) found flows involving a pendant drop hanging from the cylinder's lower part. Unlike the smooth and shock flows, the loads of the pendant-drop flows

† Email address for correspondence: eugene.benilov@ul.ie

https://doi.org/10.1017/jfm.2013.530 Published online by Cambridge University Press

are unbounded, which suggests that the maximum load may not be determined by a limiting solution. Alternatively, an instability can be the limiting factor, provided it is triggered off if the load exceeds a certain threshold.

Generally, flows on a rotating horizontal cylinder are prone to two different instabilities, which were both examined for Moffatt's (1977) smooth solutions. The first instability, of a Taylor–Goldstein kind, results from hydrostatic destabilization of the liquid on the cylinder's lower half by gravity (Benilov, O'Brien & Sazonov 2003; Benilov 2004). The second instability is caused by the liquid's inertia (Benilov & O'Brien 2005; Pougatch & Frigaard 2011).

The mere fact that Moffatt's (1977) smooth flows are unstable, and that their loads are smaller than those of the other solutions, has important physical implications. It suggests that, apart from the maximum load, there exists, surprisingly, a minimum one. In other words, if an amount of liquid on a cylinder is smaller than a certain threshold value, it cannot form a steady state. One can conjecture that, if the instability develops sufficiently fast, part of the liquid would fall off the cylinder, with the remaining part forming three-dimensional 'rings' (Leslie, Wilson & Duffy 2013).

Note, however, that both above instabilities have been studied using the lubrication approximation (LA), which is inapplicable to perturbations with wavelengths comparable to, or shorter than, the depth of the liquid layer. The *long*-wave instability, in turn, *can* be studied using the LA, but is usually relatively weak. This can be illustrated by the above-mentioned result of Benilov & O'Brien (2005) – who used the LA to show that the growth rate of the inertial instability increases with the perturbation's wavenumber, with an implication that the strongest instability occurs beyond the limits of the LA. We might also mention that the LA can give rise to 'spurious' instabilities, which do not exist in more accurate models (O'Brien 2002; Benilov, Kopteva & O'Brien 2005), as well as spurious steady states, including some of the above-mentioned shock solutions (see Benilov & Lapin 2011; Benilov, Lapin & O'Brien 2012). Thus, even though Moffatt's (1977) low-load solutions are unstable, it is unclear whether the instability is fast enough to make the honey drip down from the spoon.

Note also that, even though Moffatt's (1977) original study was motivated by scientific curiosity in its purest form, coating and rimming flows have many industrial applications – such as rotational moulding (Throne & Gianchandani 1980), coating of fluorescent light bulbs (O'Brien 1998), or modelling of aero-engines (Williams *et al.* 2012). In most applications, the instability is undesirable (for example, it makes the coating on fluorescent tubes uneven, etc.).

In the present paper, we use the full Navier–Stokes equations to examine the stability of coating and rimming flows described by Moffatt's (1977) solutions, with respect to short-wave disturbances. Such disturbances do not satisfy the LA, but the base state still does, which noticeably simplifies our task.

This paper has the following structure. In § 2, we introduce the governing equations and, in § 3, discuss the non-dimensional parameters involved. In § 4, a set of asymptotic equations for a disturbance in a steady flow is derived. In § 5, we consider the case of Stokes flow, which is the simplest non-LA model (it allows for short-wave disturbances but still ignores inertia). In § 6, we shall examine the general case, revealing the mechanisms of an instability due to inertial effects. In § 7, we summarize the results and discuss their implications for the problem of honey on a rotating spoon.

https://doi.org/10.1017/jfm.2013.530 Published online by Cambridge University Press

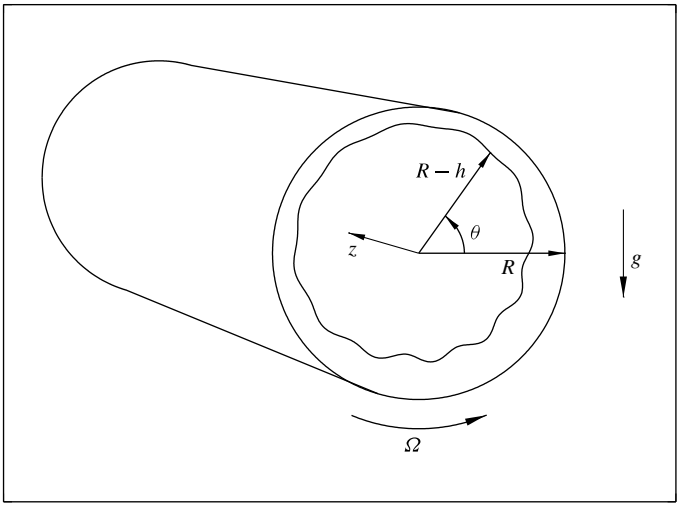

FIGURE 1. Liquid film in a rotating horizontal cylinder.

2. Formulation of the problem

As mentioned above, even though the governing sets of equations for coating and rimming flows are different, the asymptotic results obtained for thin films are usually applicable to both (not only qualitatively, but also quantitatively). The present problem is not an exception in this respect, so the details of the analysis will be presented only for rimming flows.

Consider a thin layer of liquid on the inside surface of an infinitely long cylinder of radius R (see figure 1). The axis of the cylinder is horizontal, and it is rotating about this axis with constant angular velocity Ω. We shall use cylindrical coordinates (r, θ, z), so the thickness h of the film depends on the azimuthal angle θ, axial coordinate z and time t. In addition to h, the flow is characterized by the radial, angular and axial velocities, u, v and w, respectively, and the pressure p (the fluid is assumed incompressible, so its density, ρ, is constant).

In cylindrical coordinates, the Navier–Stokes equations are (Landau & Lifshitz 1995)

$$\frac{\partial u}{\partial t} + u\frac{\partial u}{\partial r} + \frac{v}{r}\left(\frac{\partial u}{\partial \theta} - v\right) + w\frac{\partial u}{\partial z} + \frac{1}{\rho}\frac{\partial p}{\partial r} = -g\sin\theta + \nu\left[\frac{\partial^2 u}{\partial r^2} + \frac{1}{r}\frac{\partial u}{\partial r} + \frac{1}{r^2}\left(\frac{\partial^2 u}{\partial \theta^2} - u - 2\frac{\partial v}{\partial \theta}\right) + \frac{\partial^2 u}{\partial z^2}\right], \tag{2.1}$$

$$\frac{\partial v}{\partial t} + u\frac{\partial v}{\partial r} + \frac{v}{r}\left(\frac{\partial v}{\partial \theta} + u\right) + w\frac{\partial v}{\partial z} + \frac{1}{\rho r}\frac{\partial p}{\partial \theta} = -g\cos\theta + \nu\left[\frac{\partial^2 v}{\partial r^2} + \frac{1}{r}\frac{\partial v}{\partial r} + \frac{1}{r^2}\left(\frac{\partial^2 v}{\partial \theta^2} - v + 2\frac{\partial u}{\partial \theta}\right) + \frac{\partial^2 v}{\partial z^2}\right], \tag{2.2}$$

$$\frac{\partial w}{\partial t} + u\frac{\partial w}{\partial r} + \frac{v}{r}\frac{\partial w}{\partial \theta} + w\frac{\partial w}{\partial z} + \frac{1}{\rho r}\frac{\partial p}{\partial z} = \nu\left(\frac{\partial^2 w}{\partial r^2} + \frac{1}{r}\frac{\partial w}{\partial r} + \frac{1}{r^2}\frac{\partial^2 w}{\partial \theta^2} + \frac{\partial^2 w}{\partial z^2}\right), \tag{2.3}$$

https://doi.org/10.1017/jfm.2013.530 Published online by Cambridge University Press

$$\frac{\partial u}{\partial r}+\frac{1}{r}\left(u+\frac{\partial v}{\partial \theta}\right)+\frac{\partial w}{\partial z}=0, \tag{2.4}$$

where g is the acceleration due to gravity and ν is the kinematic viscosity. These equations should be supplemented by the boundary conditions at the surface of the cylinder,

$$u=0, \quad v=\Omega R, \quad w=0 \quad \text{at } r=R, \tag{2.5}$$

and the kinematic boundary condition at the film's free surface,

$$\frac{\partial h}{\partial t}+\frac{v}{r}\frac{\partial h}{\partial \theta}+w\frac{\partial h}{\partial z}+u=0 \quad \text{at } r=R-h. \tag{2.6}$$

We shall also require that the two tangential components of the stress tensor $\boldsymbol{S}$ at the free surface are zero, whereas the normal component is proportional to the curvature of the surface. All these requirements can be written as a single vector condition,

$$(\boldsymbol{S}-\sigma C\boldsymbol{I})\boldsymbol{n}=\boldsymbol{0} \quad \text{at } r=R-h, \tag{2.7}$$

where σ is the surface tension coefficient, $\boldsymbol{I}$ is the identity matrix, $\boldsymbol{n}$ is a normal (not necessarily unit) to the free surface, and

$$C=\frac{(R-h)^2+(R-h)\dfrac{\partial^2 h}{\partial\theta^2}+(R-h)^3\dfrac{\partial^2 h}{\partial z^2}+2\left(\dfrac{\partial h}{\partial\theta}\right)^2+(R-h)^2\left(\dfrac{\partial h}{\partial z}\right)^2}{\left[(R-h)^2+\left(\dfrac{\partial h}{\partial\theta}\right)^2+(R-h)^2\left(\dfrac{\partial h}{\partial z}\right)^2\right]^{3/2}}$$
$$+\frac{(R-h)\left[\left(\dfrac{\partial h}{\partial z}\right)^2\dfrac{\partial^2 h}{\partial\theta^2}-2\dfrac{\partial h}{\partial\theta}\dfrac{\partial h}{\partial z}\dfrac{\partial^2 h}{\partial z\,\partial\theta}+\left(\dfrac{\partial h}{\partial\theta}\right)^2\dfrac{\partial^2 h}{\partial z^2}\right]}{\left[(R-h)^2+\left(\dfrac{\partial h}{\partial\theta}\right)^2+(R-h)^2\left(\dfrac{\partial h}{\partial z}\right)^2\right]^{3/2}} \tag{2.8}$$

is the curvature of the film's surface (Finn 1986). Expressing $\boldsymbol{n}$ and $\boldsymbol{S}$ in terms of the cylindrical coordinates (e.g. Landau & Lifshitz 1995) and substituting them into (2.7), we obtain

$$2\frac{\partial u}{\partial r}-\frac{p+\sigma C}{\rho\nu}+\left[\frac{1}{r}\left(\frac{\partial u}{\partial\theta}-v\right)+\frac{\partial v}{\partial r}\right]\frac{1}{R-h}\frac{\partial h}{\partial\theta}$$
$$+\left(\frac{\partial u}{\partial z}+\frac{\partial w}{\partial r}\right)\frac{\partial h}{\partial z}=0 \quad \text{at } r=R-h, \tag{2.9}$$

$$\frac{1}{r}\left(\frac{\partial u}{\partial\theta}-v\right)+\frac{\partial v}{\partial r}+\left[\frac{2}{r}\left(\frac{\partial v}{\partial\theta}+u\right)-\frac{p+\sigma C}{\rho\nu}\right]\frac{1}{R-h}\frac{\partial h}{\partial\theta}$$
$$+\left(\frac{\partial v}{\partial z}+\frac{1}{r}\frac{\partial w}{\partial\theta}\right)\frac{\partial h}{\partial z}=0 \quad \text{at } r=R-h, \tag{2.10}$$

$$\frac{\partial u}{\partial z}+\frac{\partial w}{\partial r}+\left(\frac{\partial v}{\partial z}+\frac{1}{r}\frac{\partial w}{\partial\theta}\right)\frac{1}{R-h}\frac{\partial h}{\partial\theta}$$
$$+\left(2\frac{\partial w}{\partial z}-\frac{p+\sigma C}{\rho\nu}\right)\frac{\partial h}{\partial z}=0 \quad \text{at } r=R-h. \tag{2.11}$$

https://doi.org/10.1017/jfm.2013.530 Published online by Cambridge University Press

Given suitable initial conditions, equations (2.1)–(2.6) and (2.8)–(2.11) determine the unknowns u, v, w, p and h.

3. The non-dimensional parameters

The evolution of a coating or rimming flow with a characteristic thickness $\langle h\rangle$ is governed by five non-dimensional parameters. Four of those are associated with the physical setting:

$$\delta = \frac{\langle h\rangle}{R} \tag{3.1}$$

is the non-dimensional thickness of the film,

$$\alpha = \frac{\langle h\rangle R\Omega}{\nu} \tag{3.2}$$

is an effective Reynolds number (based on the spatial scale $\langle h\rangle$ and velocity scale ΩR),

$$\lambda = \frac{g\langle h\rangle^2}{R\Omega\nu} \tag{3.3}$$

is the ratio of the gravitational and viscous forces, and

$$\gamma = \frac{\sigma}{\rho\Omega R\nu} \tag{3.4}$$

is the ratio of the capillary and viscous forces. The fifth parameter characterizes the spatial structure of the flow,

$$\Delta = \frac{\langle h\rangle}{\min\{R\Delta\theta,\, \Delta z\}}, \tag{3.5}$$

where $\Delta\theta$ and Δz are the azimuthal and axial scales. In what follows, Δ will be referred to as the 'aspect ratio'.

We shall define the LA by

$$\delta \ll 1, \tag{3.6}$$

$$\Delta \ll 1, \tag{3.7}$$

$$\lambda \lesssim 1, \tag{3.8}$$

$$\alpha\Delta \ll 1, \tag{3.9}$$

$$\gamma\Delta^3 \lesssim 1. \tag{3.10}$$

To clarify the physical meaning of these requirements, note the following:

(*a*) The thin-film condition (3.6) allows the cylindrical geometry of the problem to be approximated by the Cartesian one.

(*b*) The shallow-water condition (3.7) makes the dynamic component of the pressure field small – as a result, the leading-order pressure is determined by the hydrostatic formula. Equation (3.7) makes also the 'azimuthal' friction stronger than the 'radial' one.

(*c*) Condition (3.8) guarantees that gravity does not dominate viscous entrainment. If it did, fluid would accumulate in a pool at the bottom of the cylinder, with virtually no film on its walls.

https://doi.org/10.1017/jfm.2013.530 Published online by Cambridge University Press

(*d*) Condition (3.9) guarantees that viscous entrainment of the fluid by the cylinder's rotation dominates inertia (the latter is described by the material derivatives in the Navier–Stokes equations).

(*e*) Condition (3.10) guarantees that, for flows with spatial scales comparable to R, surface tension does not dominate viscosity. Note, however, that, for most fluids, surface tension is weak (see the example below) and (3.10) can be safely replaced with a stronger condition,

$$\gamma \Delta^3 \ll 1. \tag{3.11}$$

To illustrate restrictions (3.6)–(3.9) and (3.11), consider the following example. Let the fluid under consideration be glycerine at 20 °C, for which

$$\nu = 1.12 \times 10^{-3}\ \mathrm{m^2\ s^{-1}}, \quad \sigma = 0.063\ \mathrm{N\ m^{-1}}, \quad \rho = 1.26 \times 10^3\ \mathrm{kg\ m^{-3}}. \tag{3.12}$$

The angular velocity of the cylinder, its radius and the film's thickness are taken to be

$$\Omega = 2\pi\ \mathrm{s^{-1}}, \quad R = 0.03\ \mathrm{m}, \quad \langle h \rangle = 0.003\ \mathrm{m}. \tag{3.13}$$

Substitution of (3.12) and (3.13) into (3.1)–(3.4) yields

$$\delta = 0.1, \quad \alpha \approx 0.51, \quad \lambda \approx 0.42, \quad \gamma \approx 0.24. \tag{3.14}$$

Observe that $\delta \ll 1$ and $\lambda \sim 1$ – hence, the film is thin and gravity is on par with viscous entrainment.

To assess the impact of inertia and surface tension, observe that a steady rimming flow varies on the scale of the cylinder, i.e. $\Delta\theta = 1$, $\Delta z = R$. Then, (3.5) yields for the aspect ratio $\Delta = \delta$, and

$$\alpha\Delta = 0.051, \quad \gamma\Delta^3 = 0.000\,24. \tag{3.15}$$

Clearly, conditions (3.9) and (3.11) hold, which means that, for steady rimming flows, inertia and surface tension are negligible.

Next, consider a short-wave disturbance, with a wavelength comparable to the film's thickness, i.e. $\Delta\theta = \langle h \rangle / R$, $\Delta z = \langle h \rangle$. In this case, (3.5) yields $\Delta = 1$. Then, we obtain

$$\alpha\Delta = 0.51, \quad \gamma\Delta^3 = 0.24, \tag{3.16}$$

and conditions (3.9) and (3.11) do *not* hold. This indicates that the impact of inertia and surface tension on such a disturbance is comparable to that of viscosity.

Thus, even though the inertial effects and surface tension are negligible for the steady state, they must be retained for disturbances, and the LA may not be used for them.

4. The analysis

In this section, we shall derive asymptotic equations for the steady state (§ 4.1), and those for the disturbance (§ 4.2).

4.1. *The steady state*

Assume that the flow satisfies the LA, which implies the following non-dimensional variables:

$$\tilde{r} = \frac{R - r}{\delta R}, \quad \tilde{\theta} = \theta, \quad \tilde{z} = \frac{z}{R}, \quad \tilde{t} = \Omega t, \tag{4.1}$$

https://doi.org/10.1017/jfm.2013.530 Published online by Cambridge University Press

$$\tilde{u} = -\frac{u}{\delta R\Omega}, \quad \tilde{v} = \frac{v}{R\Omega}, \quad \tilde{w} = \frac{w}{R\Omega}, \quad \tilde{p} = \frac{\delta}{\rho\nu\Omega}\left(p + \frac{\sigma}{R}\right), \tag{4.2}$$

$$\tilde{h} = \frac{h}{\delta R}, \quad \tilde{C} = \frac{CR - 1}{\delta}, \tag{4.3}$$

where, as before, δ is the ratio of the film's thickness to the cylinder's radius. Note that the σ/R term in the expression for $\widetilde{p}$ and the -1 in the expression for $\widetilde{C}$ represent capillary effects associated with the cylinder's curvature.

In terms of the new variables, (2.1)–(2.6), (2.9)–(2.11) and (2.8) become (tildes omitted)

$$\alpha\delta\left[\delta\frac{\partial u}{\partial t} + \delta u\frac{\partial u}{\partial r} + \frac{v}{1-\delta r}\left(\delta\frac{\partial u}{\partial\theta} + v\right) + \delta w\frac{\partial u}{\partial z}\right] + \frac{\partial p}{\partial r}$$
$$= \lambda\sin\theta + \delta\left[\frac{\partial^2 u}{\partial r^2} - \frac{\delta}{1-\delta r}\frac{\partial u}{\partial r} + \frac{\delta}{(1-\delta r)^2}\left(\delta\frac{\partial^2 u}{\partial\theta^2} - \delta u + 2\frac{\partial v}{\partial\theta}\right) + \delta^2\frac{\partial^2 u}{\partial z^2}\right], \tag{4.4}$$

$$\alpha\delta\left[\frac{\partial v}{\partial t} + u\frac{\partial v}{\partial r} + \frac{v}{1-\delta r}\left(\frac{\partial v}{\partial\theta} - \delta u\right) + w\frac{\partial v}{\partial z}\right] + \frac{\delta}{1-\delta r}\frac{\partial p}{\partial\theta}$$
$$= -\cos\theta + \frac{\partial^2 v}{\partial r^2} - \frac{\delta}{1-\delta r}\frac{\partial v}{\partial r} + \frac{\delta^2}{(1-\delta r)^2}\left(\frac{\partial^2 v}{\partial\theta^2} - v - 2\delta\frac{\partial u}{\partial\theta}\right) + \delta^2\frac{\partial^2 v}{\partial z^2}, \tag{4.5}$$

$$\alpha\delta\left(\frac{\partial w}{\partial t} + u\frac{\partial w}{\partial r} + \frac{v}{1-\delta r}\frac{\partial w}{\partial\theta} + w\frac{\partial w}{\partial z}\right) + \delta\frac{\partial p}{\partial z}$$
$$= \frac{\partial^2 w}{\partial r^2} - \frac{\delta}{1-\delta r}\frac{\partial w}{\partial r} + \frac{\delta^2}{(1-\delta r)^2}\frac{\partial^2 w}{\partial\theta^2} + \delta^2\frac{\partial^2 w}{\partial z^2}, \tag{4.6}$$

$$(1-\delta r)\frac{\partial u}{\partial r} - \delta u + \frac{\partial v}{\partial\theta} + (1-\delta r)\frac{\partial w}{\partial z} = 0, \tag{4.7}$$

$$u = 0, \quad v = 1, \quad w = 0 \quad \text{at } r = 0, \tag{4.8}$$

$$\frac{\partial h}{\partial t} + \frac{v}{1-\delta h}\frac{\partial h}{\partial\theta} + w\frac{\partial h}{\partial z} - u = 0 \quad \text{at } r = h, \tag{4.9}$$

$$2\delta\frac{\partial u}{\partial r} - p - \gamma\delta^2 C - \left[\frac{\delta}{1-\delta h}\left(\delta\frac{\partial u}{\partial\theta} + v\right) + \frac{\partial v}{\partial r}\right]\frac{\delta}{1-\delta h}\frac{\partial h}{\partial\theta}$$
$$-\delta\left(\delta^2\frac{\partial u}{\partial z} + \frac{\partial w}{\partial r}\right)\frac{\partial h}{\partial z} = 0 \quad \text{at } r = h, \tag{4.10}$$

$$\delta\left(\delta\frac{\partial u}{\partial\theta} + v\right) + \frac{\partial v}{\partial r} - \left[\frac{2\delta}{1-\delta h}\left(\delta\frac{\partial v}{\partial\theta} - u\right) - p - \gamma\delta^2 C\right]\frac{\delta}{1-\delta h}\frac{\partial h}{\partial\theta}$$
$$-\delta^2\left(\frac{\partial v}{\partial z} + \frac{1}{r}\frac{\partial w}{\partial\theta}\right)\frac{\partial h}{\partial z} = 0 \quad \text{at } r = h, \tag{4.11}$$

$$\delta^2\frac{\partial u}{\partial z} + \frac{\partial w}{\partial r} - \left(\frac{\partial v}{\partial z} + \frac{1}{1-\delta h}\frac{\partial w}{\partial\theta}\right)\frac{\delta^2}{1-\delta h}\frac{\partial h}{\partial\theta}$$
$$-\delta\left(2\delta\frac{\partial w}{\partial z} - p - \gamma\delta^2 C\right)\frac{\partial h}{\partial z} = 0 \quad \text{at } r = h, \tag{4.12}$$

https://doi.org/10.1017/jfm.2013.530 Published online by Cambridge University Press

$$C = \frac{(1-\delta h)^2 + \delta(1-\delta h)\dfrac{\partial^2 h}{\partial\theta^2} + \delta(1-\delta h)^3\dfrac{\partial^2 h}{\partial z^2} + 2\delta^2\left(\dfrac{\partial h}{\partial\theta}\right)^2 + \delta^2(1-\delta h)^2\left(\dfrac{\partial h}{\partial z}\right)^2}{\delta\left[(1-\delta h)^2 + \delta^2\left(\dfrac{\partial h}{\partial\theta}\right)^2 + \delta^2(1-\delta h)^2\left(\dfrac{\partial h}{\partial z}\right)^2\right]^{3/2}}$$
$$- \frac{1}{\delta} + \frac{\delta^2(1-\delta h)\left[\left(\dfrac{\partial h}{\partial z}\right)^2\dfrac{\partial^2 h}{\partial\theta^2} - 2\dfrac{\partial h}{\partial\theta}\dfrac{\partial h}{\partial z}\dfrac{\partial^2 h}{\partial z\,\partial\theta} + \left(\dfrac{\partial h}{\partial\theta}\right)^2\dfrac{\partial^2 h}{\partial z^2}\right]}{\left[(1-\delta h)^2 + \delta^2\left(\dfrac{\partial h}{\partial\theta}\right)^2 + \delta^2(1-\delta h)^2\left(\dfrac{\partial h}{\partial z}\right)^2\right]^{3/2}}, \tag{4.13}$$

where α, λ and γ are determined by (3.2)–(3.4) with $\langle h\rangle = \delta R$. Observe also that scaling (4.1) implies that the azimuthal and axial scales of the solution are $\Delta\theta = 1$ and $\Delta z = R$ – which is, essentially, the steady-state scaling.

Now, seek a steady, axially homogeneous solution, i.e. put

$$u = \bar{u}(r,\theta), \quad v = \bar{v}(r,\theta), \quad w = 0, \quad p = \bar{p}(r,\theta), \quad h = \bar{h}(\theta). \tag{4.14}$$

Assuming that $\delta \ll 1$, whereas $\alpha, \lambda, \gamma \sim 1$, substitute (4.14) into (4.4)–(4.13) and keep the leading-order terms only:

$$\frac{\partial\bar{p}}{\partial r} = \lambda\sin\theta, \quad 0 = -\lambda\cos\theta + \frac{\partial^2\bar{v}}{\partial r^2}, \quad \frac{\partial\bar{u}}{\partial r} + \frac{\partial\bar{v}}{\partial\theta} = 0, \tag{4.15}$$

$$\bar{u} = 0, \quad \bar{v} = 1 \quad \text{at } r = 0, \tag{4.16}$$

$$v\frac{\partial h}{\partial\theta} - u = 0 \quad \text{at } r = h, \tag{4.17}$$

$$\bar{p} = 0, \quad \frac{\partial\bar{v}}{\partial r} = 0 \quad \text{at } r = h. \tag{4.18}$$

Using (4.15), (4.16) and (4.18), one can express $\bar{p}$, $\bar{v}$ and $\bar{u}$ in terms of $\bar{h}$,

$$\bar{p} = \lambda(r - \bar{h})\sin\theta, \tag{4.19}$$

$$\bar{v} = 1 + \lambda\left(\frac{r^2}{2} - r\bar{h}\right)\cos\theta, \tag{4.20}$$

$$\bar{u} = \frac{\lambda r^2}{2}\left[\frac{\partial\bar{h}}{\partial\theta}\cos\theta - \left(\bar{h} - \frac{r}{3}\right)\sin\theta\right]. \tag{4.21}$$

Next, substitute (4.20) and (4.21) into (4.17) and integrate the latter with respect to θ, which yields

$$\bar{h} - \frac{\lambda\bar{h}^3}{3}\cos\theta = \text{const}. \tag{4.22}$$

Without loss of generality, we can assume that the scale $\langle h\rangle$ for the variable $\bar{h}$ is such that the constant of integration in the above equation is equal to unity, so we have

$$\bar{h} - \frac{\lambda\bar{h}^3}{3}\cos\theta = 1. \tag{4.23}$$

https://doi.org/10.1017/jfm.2013.530 Published online by Cambridge University Press

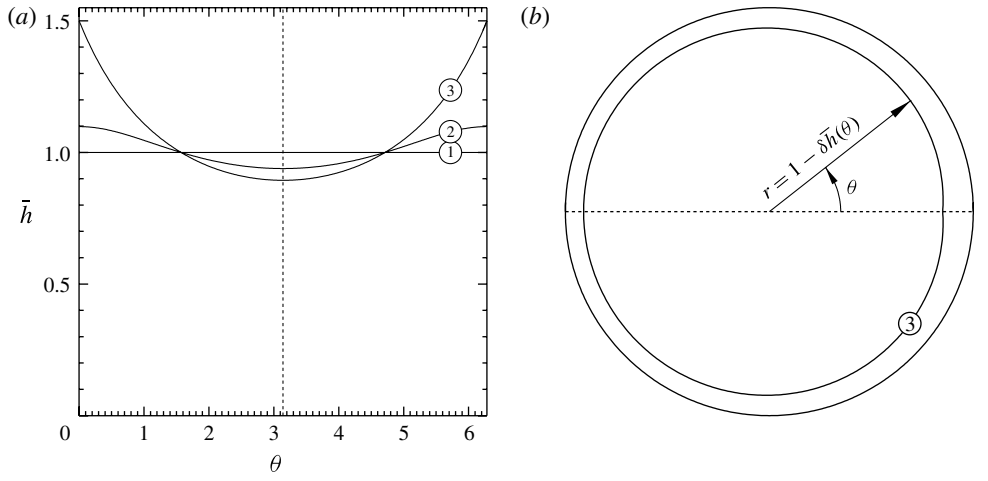

FIGURE 2. Steady rimming flows (solutions of (4.23)) for ① $\lambda = 0$, ② $\lambda = 2/9$ and ③ $\lambda = 4/9$. (*a*) The Cartesian representation; (*b*) the cylindrical representation ($\delta = 0.1$, the dotted line shows the axis of symmetry).

This (cubic) equation was examined by Moffatt (1977), who demonstrated that, if $\lambda < 4/9$, it has a smooth unique solution for $\bar{h}(\theta)$ – see figure 2. Observe that

$$\bar{h}\left(\pm\frac{\pi}{2}\right) = 1, \tag{4.24}$$

which implies that the dimensional scale $\langle h\rangle$ can be identified with the film's thickness at $\theta = \pm\pi/2$ (i.e. at the bottom or top of the cylinder).

Note also that, for $\lambda = 4/9$, $\bar{h}(\theta)$ has a corner at $\theta = 0$ – which can be regularized by taking into account either non-LA corrections (Wilson, Hunt & Duffy 2002) or surface tension (Ashmore *et al.* 2003; Benilov *et al.* 2008). In this work, we shall assume that λ is *not* close to 4/9, and the steady state is sufficiently smooth.

4.2. *Disturbances*

Seek a solution of (4.4)–(4.13) in the form

$$u = \bar{u}(r,\theta) + u'(t,r,\theta,z), \quad v = \bar{v}(r,\theta) + v'(t,r,\theta,z), \quad w = w'(t,r,\theta,z), \tag{4.25}$$

$$p = \bar{p}(r,\theta) + p'(t,r,\theta,z), \quad h = \bar{h}(r,\theta) + h'(t,\theta,z), \tag{4.26}$$

where the over-bars and primes mark the steady state and disturbance, respectively. Note that, for the latter,

$$\Delta\theta = \delta, \quad \Delta z = \delta R. \tag{4.27}$$

Next, the solution (4.25) and (4.26) should be substituted into the governing equations (4.4)–(4.13), which should then be linearized and rescaled in accordance with (4.27). The sheer size and number of the equations involved make this straightforward procedure impossible to present in a reasonably sized paper. Instead, we shall present its final result and explain how it has been obtained.

One can readily 'select' large terms by simply keeping in mind that, for the disturbance,

$$v' = O(1), \quad \frac{\partial v'}{\partial t}, \frac{\partial v'}{\partial\theta}, \frac{\partial v'}{\partial z} = O(\delta^{-1}), \quad \frac{\partial^2 v'}{\partial\theta^2}, \frac{\partial^2 v'}{\partial z^2} = O(\delta^{-2}), \tag{4.28}$$

https://doi.org/10.1017/jfm.2013.530 Published online by Cambridge University Press

$$w' = O(1), \quad \frac{\partial w'}{\partial t}, \frac{\partial w'}{\partial \theta} \frac{\partial w'}{\partial z} = O(\delta^{-1}), \quad \frac{\partial^2 w'}{\partial \theta^2}, \frac{\partial^2 w'}{\partial z^2} = O(\delta^{-2}), \tag{4.29}$$

$$p' = O(1), \quad \frac{\partial p'}{\partial t}, \frac{\partial p'}{\partial \theta}, \frac{\partial p'}{\partial z} = O(\delta^{-1}), \quad \frac{\partial^2 p'}{\partial \theta^2}, \frac{\partial^2 p'}{\partial z^2} = O(\delta^{-2}), \tag{4.30}$$

$$h' = O(1), \quad \frac{\partial h'}{\partial t}, \frac{\partial h'}{\partial \theta}, \frac{\partial h'}{\partial z} = O(\delta^{-1}), \quad \frac{\partial^2 h'}{\partial \theta^2}, \frac{\partial^2 h'}{\partial z^2} = O(\delta^{-2}). \tag{4.31}$$

Recall also that, in the original scaling (4.2), the radial velocity u was assumed small (observe the extra δ in the first equation of (4.2)). That was a requirement of the shallow-water approximation, which we no longer use – correspondingly, u should now be scaled up, i.e. we should assume

$$u' = O(\delta^{-1}), \quad \frac{\partial u'}{\partial t}, \frac{\partial u'}{\partial \theta}, \frac{\partial u'}{\partial z} = O(\delta^{-2}), \quad \frac{\partial^2 u'}{\partial \theta^2}, \frac{\partial^2 u'}{\partial z^2} = O(\delta^{-3}). \tag{4.32}$$

Now, substitute (4.25) and (4.26) into (4.4)–(4.13) and linearize them. Then, keeping in mind (4.28)–(4.32), retain the leading-order terms only, one obtains

$$\alpha\delta^2 \left(\frac{\partial u'}{\partial t} + \bar{v} \frac{\partial u'}{\partial \theta} \right) + \frac{\partial p'}{\partial r} = \delta \left[\frac{\partial^2 u'}{\partial r^2} + \delta^2 \left(\frac{\partial^2 u'}{\partial \theta^2} + \frac{\partial^2 u'}{\partial z^2} \right) \right], \tag{4.33}$$

$$\alpha\delta \left(\frac{\partial v'}{\partial t} + u' \frac{\partial \bar{v}}{\partial r} + \bar{v} \frac{\partial v'}{\partial \theta} \right) + \delta \frac{\partial p'}{\partial \theta} = \frac{\partial^2 v'}{\partial r^2} + \delta^2 \left(\frac{\partial^2 v'}{\partial \theta^2} + \frac{\partial^2 v'}{\partial z^2} \right), \tag{4.34}$$

$$\alpha\delta \left(\frac{\partial w'}{\partial t} + \bar{v} \frac{\partial w'}{\partial \theta} \right) + \delta \frac{\partial p'}{\partial z} = \frac{\partial^2 w'}{\partial r^2} + \delta^2 \left(\frac{\partial^2 w'}{\partial \theta^2} + \frac{\partial^2 w'}{\partial z^2} \right), \tag{4.35}$$

$$\frac{\partial u'}{\partial r} + \frac{\partial v'}{\partial \theta} + \frac{\partial w'}{\partial z} = 0, \tag{4.36}$$

$$u' = v' = w' = 0 \quad \text{at } r = 0, \tag{4.37}$$

$$\frac{\partial h'}{\partial t} + \bar{v} \frac{\partial h'}{\partial \theta} - u' = 0 \quad \text{at } r = \bar{h}, \tag{4.38}$$

$$2\delta \frac{\partial u'}{\partial r} - p' - \frac{\partial \bar{p}}{\partial r} h' - \gamma\delta^2 \left(\frac{\partial^2 h'}{\partial \theta^2} + \frac{\partial^2 h'}{\partial z^2} \right) - \delta \frac{\partial \bar{v}}{\partial r} \frac{\partial h'}{\partial \theta} = 0 \quad \text{at } r = \bar{h}, \tag{4.39}$$

$$\delta^2 \frac{\partial u'}{\partial \theta} + \frac{\partial v'}{\partial r} + \frac{\partial^2 \bar{v}}{\partial r^2} h' + \bar{p} \frac{\partial h'}{\partial \theta} = 0 \quad \text{at } r = \bar{h}, \tag{4.40}$$

$$\delta^2 \frac{\partial u'}{\partial z} + \frac{\partial w'}{\partial r} + \delta \bar{p} \frac{\partial h'}{\partial z} = 0 \quad \text{at } r = \bar{h}. \tag{4.41}$$

Note that the terms involving $\partial\bar{p}/\partial r$, $\partial\bar{v}/\partial r$ and $\partial^2\bar{v}/\partial r^2$ in (4.39) and (4.40) appeared due to the linearization of the free-surface conditions, i.e. shifting them from $r = \bar{h} + h'$ to $r = \bar{h}$.

In this paper, we shall confine ourselves to the *eigenmodes* of (4.33)–(4.41), i.e. solutions with harmonic dependence on the time variable and axial coordinate,

$$u'(t, r, \theta, z) = \frac{U(r, \theta)}{\delta} \exp\left(\frac{\mathrm{i}lz - \mathrm{i}\omega t}{\delta} \right), \tag{4.42}$$

$$v' = V(r, \theta) \exp\left(\frac{\mathrm{i}lz - \mathrm{i}\omega t}{\delta} \right), \quad w' = W(r, \theta) \exp\left(\frac{\mathrm{i}lz - \mathrm{i}\omega t}{\delta} \right), \tag{4.43}$$

$$p' = P(r, \theta) \exp\left(\frac{\mathrm{i}lz - \mathrm{i}\omega t}{\delta} \right), \quad h' = H(\theta) \exp\left(\frac{\mathrm{i}lz - \mathrm{i}\omega t}{\delta} \right), \tag{4.44}$$

https://doi.org/10.1017/jfm.2013.530 Published online by Cambridge University Press

where l/δ is the axial wavenumber, ω/δ is the frequency, and the factor δ^{-1} in (4.42) reflects that we no longer use the LA and u' is not small. Such scaling assumes the axial wavelength to be comparable to the film's thickness and the frequency to exceed the angular velocity of the cylinder by a factor of δ^{-1}.

Now substitute (4.42)–(4.44) into (4.33)–(4.41), and take into account that

$$\frac{\partial \bar{p}}{\partial r} = \lambda \sin\theta, \quad \frac{\partial \bar{v}}{\partial r} = 0, \quad \frac{\partial^2 \bar{v}}{\partial r^2} = \lambda \cos\theta, \quad \bar{v} = 1 - \frac{\lambda \bar{h}^2}{2}\cos\theta \quad \text{at } r = \bar{h} \tag{4.45}$$

(these formulae follow from (4.19) and (4.20)). Doing so, we obtain

$$\alpha\left(-\mathrm{i}\omega U + \delta\bar{v}\frac{\partial U}{\partial\theta}\right) + \frac{\partial P}{\partial r} = \frac{\partial^2 U}{\partial r^2} + \delta^2\frac{\partial^2 U}{\partial\theta^2} - l^2 U, \tag{4.46}$$

$$\alpha\left(-\mathrm{i}\omega V + U\frac{\partial \bar{v}}{\partial r} + \delta\bar{v}\frac{\partial V}{\partial\theta}\right) + \delta\frac{\partial P}{\partial\theta} = \frac{\partial^2 V}{\partial r^2} + \delta^2\frac{\partial^2 V}{\partial\theta^2} - l^2 V, \tag{4.47}$$

$$\alpha\left(-\mathrm{i}\omega W + \delta\bar{v}\frac{\partial W}{\partial\theta}\right) + \mathrm{i}lP = \frac{\partial^2 W}{\partial r^2} + \delta^2\frac{\partial^2 W}{\partial\theta^2} - l^2 W, \tag{4.48}$$

$$\frac{\partial U}{\partial r} + \delta\frac{\partial V}{\partial\theta} + \mathrm{i}lW = 0, \tag{4.49}$$

$$U = 0, \quad V = 0, \quad W = 0 \quad \text{at } r = 0, \tag{4.50}$$

$$-\mathrm{i}\omega H + \delta\left(1 - \frac{\lambda\bar{h}^2}{2}\cos\theta\right)\frac{\partial H}{\partial\theta} - U = 0 \quad \text{at } r = \bar{h}, \tag{4.51}$$

$$2\frac{\partial U}{\partial r} - P - \gamma\left(\delta^2\frac{\partial^2 H}{\partial\theta^2} - l^2 H\right) - \lambda H\sin\theta = 0 \quad \text{at } r = \bar{h}, \tag{4.52}$$

$$\delta\frac{\partial U}{\partial\theta} + \frac{\partial V}{\partial r} + \lambda H\cos\theta = 0 \quad \text{at } r = \bar{h}, \tag{4.53}$$

$$\mathrm{i}lU + \frac{\partial W}{\partial r} = 0 \quad \text{at } r = \bar{h}. \tag{4.54}$$

The boundary-value problem (4.46)–(4.54) determines the unknowns U, V, W, P and H. The steady-state characteristics $\bar{v}(\theta, r)$ and $\bar{h}(\theta)$ play the role of coefficients and are determined by (4.20) and (4.23).

4.3. *Discussion*

Generally, (4.46)–(4.54) describe linear gravity–capillary waves in a layer of variable thickness and velocity, with gravity gradually changing its direction. The geometry of the problem has become Cartesian, as the effect of cylindricity is weak (recall that the thickness of the film and the wavelength of the disturbance are both smaller than the radius of the cylinder). Note, however, that our equations are noticeably simpler than the full linearized Navier–Stokes set, as some of the terms have been omitted due to the fact that the steady state satisfies the LA.

Note also that the corresponding set of equations for coating flows can be obtained from the rimming-flow set (4.46)–(4.54) by changing $H \to -H$, $r \to -r$ and $U \to -U$.

Finally, note that the Wentzel–Kramers–Brillouin (WKB) method is expected to fail in the limit $\lambda \to 4/9$, when a 'corner' appears on the film's surface. In this case, the spatial scale of the steady state cannot be assumed to be larger than that of the disturbance.

https://doi.org/10.1017/jfm.2013.530 Published online by Cambridge University Press

5. The Stokes-flow limit

In this section, we shall examine the limit $\alpha \to 0$. It will be used for testing the asymptotic method later applied to the general case, and also for physical interpretation of the results obtained. We shall also clarify the effect of the non-LA corrections on the exploding solutions found in this problem previously (Benilov *et al.* 2003; Benilov 2004; Benilov, Lacey & O'Brien 2005) and the instability found by O'Brien (2002) and Benilov *et al.* (2005).

5.1. *The eigenmodes*

In this case, the first three equations of the set (4.46)–(4.54) become

$$\frac{\partial P}{\partial r} = \frac{\partial^2 U}{\partial r^2} + \delta^2 \frac{\partial^2 U}{\partial \theta^2} - l^2 U, \quad \delta \frac{\partial P}{\partial \theta} = \frac{\partial^2 V}{\partial r^2} + \delta^2 \frac{\partial^2 V}{\partial \theta^2} - l^2 V, \tag{5.1}$$

$$\mathrm{i}lP = \frac{\partial^2 W}{\partial r^2} + \delta^2 \frac{\partial^2 W}{\partial \theta^2} - l^2 W. \tag{5.2}$$

Observe that (5.1) and (5.2) reflect the balance of the pressure gradient and viscosity, which is often referred to as the *Stokes-flow approximation*.

Together with the periodicity condition in θ, equations (5.1), (5.2) and (4.49)–(4.54) form an eigenvalue problem for the eigenfrequency ω (if $\mathrm{Im}\,\omega > 0$, the flow is unstable). Unfortunately, the problem is too complicated to be solved exactly, as it involves variable coefficients and a curved boundary – however, it also involves the small parameter δ and, thus, can be analysed asymptotically.

Observe that, in (5.1), (5.2) and (4.49)–(4.54), δ always appears next to a derivative with respect to θ. This suggests using a suitable WKB technique – in fact, we can take advantage of the asymptotic method developed by Benilov *et al.* (2003) for the LA equivalent of the present problem. According to this method (adopted to the problem in hand), the solution can be represented by

$$U(r,\theta) = \hat{U}(r,\theta)\, \exp\left[\frac{\mathrm{i}}{\delta}\int_0^\theta m(\theta')\,\mathrm{d}\theta'\right], \quad V(r,\theta) = \cdots, \quad \ldots \tag{5.3}$$

where $m(\theta)$ is the 'local' azimuthal wavenumber, varying with θ. The functions $\hat{U}$, $\hat{V}$, ... are assumed to be periodic with respect to θ – hence, the periodicity of the original unknowns U, V, ... requires

$$\frac{1}{\delta}\int_0^{2\pi} m(\theta)\,\mathrm{d}\theta = 2\pi n, \tag{5.4}$$

where n is an integer (the azimuthal mode number). We shall also expand the unknowns in powers of δ,

$$m = m^{(0)} + \delta m^{(1)} + O(\delta^2), \quad \hat{U} = \hat{u}^{(0)} + \delta \hat{u}^{(1)} + O(\delta^2), \quad \hat{V} = \cdots, \quad \ldots. \tag{5.5}$$

Substituting (5.3) and (5.5) into (5.1), (5.2) and (4.49)–(4.54), keeping the leading-order terms only, and omitting hats and superscripts, we obtain

$$\frac{\partial P}{\partial r} = \frac{\partial^2 U}{\partial r^2} - k^2 U, \tag{5.6}$$

$$\mathrm{i}mP = \frac{\partial^2 V}{\partial r^2} - k^2 V, \tag{5.7}$$

$$\mathrm{i}lP = \frac{\partial^2 W}{\partial r^2} - k^2 W, \tag{5.8}$$

https://doi.org/10.1017/jfm.2013.530 Published online by Cambridge University Press

$$\frac{\partial U}{\partial r} + \mathrm{i}(mV + lW) = 0, \tag{5.9}$$

$$U = 0, \quad V = 0, \quad W = 0 \quad \text{at } r = 0, \tag{5.10}$$

$$-\mathrm{i}\omega H + m\left(1 - \frac{\lambda \bar{h}^2}{2}\cos\theta\right) H - U = 0 \quad \text{at } r = \bar{h}, \tag{5.11}$$

$$2\frac{\partial U}{\partial r} - P - H(\sin\theta - \gamma k^2) = 0, \quad \mathrm{i}mU + \frac{\partial V}{\partial r} + H\cos\theta = 0 \quad \text{at } r = \bar{h}, \tag{5.12}$$

$$\mathrm{i}lU + \frac{\partial W}{\partial r} = 0 \quad \text{at } r = \bar{h}, \tag{5.13}$$

where

$$k^2 = m^2 + l^2. \tag{5.14}$$

The boundary-value problem (5.6)–(5.13) is solved in the Appendix, where it is shown that a solution exists if and only if

$$\frac{\omega - m}{\lambda} + \frac{m\bar{h}^2\cos\theta}{2} + \frac{mk\bar{h}^2\cos\theta - \mathrm{i}(\cosh k\bar{h}\sinh k\bar{h} - k\bar{h})(\sin\theta - \gamma k^2)}{2k(\cosh^2 k\bar{h} + k^2\bar{h}^2)} = 0. \tag{5.15}$$

5.2. *Discussion: localized wave packets versus eigenmodes*

Before we apply (5.15) to eigenmodes, it is instructive to interpret it using localized wave packets.

Consider a packet of short waves, propagating around the cylinder and currently located at a point θ. It can be demonstrated that the local parameters of the packet (axial and azimuthal wavenumbers, l/δ and m/δ, and the frequency ω/δ) are related to the local properties of the medium and to each other by the *dispersion relationship* (5.15). We shall also define the azimuthal phase speed and the growth/decay rate, for which (5.15) yields

$$\frac{\mathrm{Re}\,\omega}{m} = 1 - \frac{\lambda\bar{h}^2}{2}\left(1 + \frac{1}{\cosh^2 k\bar{h} + k^2\bar{h}^2}\right)\cos\theta, \tag{5.16}$$

$$\frac{\mathrm{Im}\,\omega}{\delta} = \frac{(\cosh k\bar{h}\sinh k\bar{h} - k\bar{h})(\lambda\sin\theta - \gamma k^2)}{2\delta k(\cosh^2 k\bar{h} + k^2\bar{h}^2)}, \tag{5.17}$$

respectively. Observe that, in the absence of surface tension ($\gamma = 0$), the growth/decay rate is positive in the upper part of the cylinder and negative in the lower part – which reflects the destabilizing/stabilizing role of the hydrostatic pressure in the former/latter cases, respectively. Observe also that surface tension reduces the region of instability and, for $\gamma k^2 > \lambda$, eliminates it completely.

Expressions (5.16) and (5.17) enable us to compare the present approach with the LA, for which $k\bar{h} \ll 1$. Expanding (5.16) and (5.17) in powers of $k\bar{h}$, we obtain

$$\frac{\mathrm{Re}\,\omega}{m} = 1 - \lambda[1 + O(k^2\bar{h}^2)]\bar{h}^2\cos\theta, \tag{5.18}$$

$$\frac{\mathrm{Im}\,\omega}{\delta} = \frac{1}{\delta k}\left[\frac{1}{3}k^3\bar{h}^3 + O(k^5\bar{h}^5)\right](\lambda\sin\theta - \gamma k^2). \tag{5.19}$$

The LA formulas (5.18) and (5.19) have been compared to the original expressions (5.16) and (5.17) – see figure 3. Note that, for $\delta = 0.1$, the LA does not work very

https://doi.org/10.1017/jfm.2013.530 Published online by Cambridge University Press

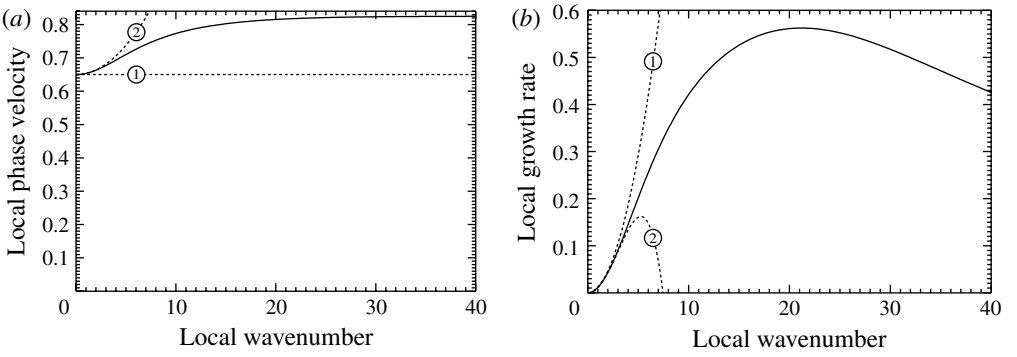

FIGURE 3. The local ($\theta = \pi/2$, $\bar{h} = 1$) dispersion relation (5.16) and (5.17) for $\delta = 0.1$, $\lambda = 0.35$ and $\gamma = 0$ (no surface tension). The corresponding LA solution is shown as the dotted lines: ①, the first-order solution (5.18) and (5.19); ②, the second-order solution (5.20) and (5.21). (*a*) The phase speed $(\mathrm{Re}\,\omega)/m$ versus the wavenumber k/δ. (*b*) The growth rate $(\mathrm{Im}\,\omega)/\delta$ versus the wavenumber k/δ.

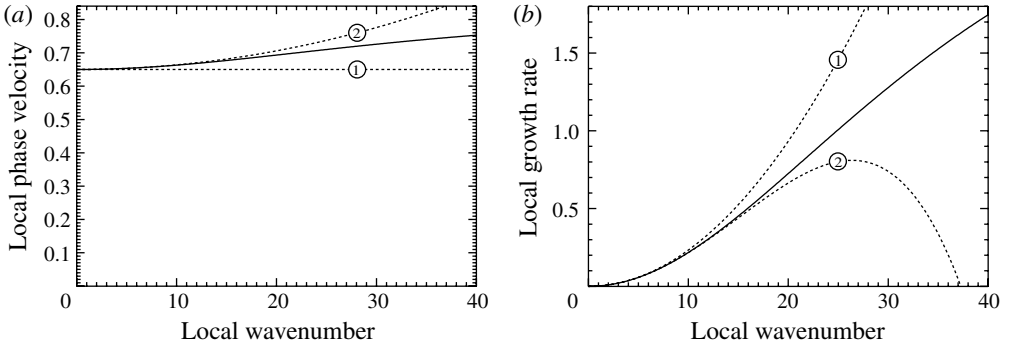

FIGURE 4. The same as figure 3, but for $\delta = 0.02$.

well, especially for the phase speed shown in figure 3(*a*); and even the next-order formulas,

$$\frac{\mathrm{Re}\,\omega}{m} = 1 - \lambda[1 - k^2\bar{h}^2 + O(k^4\bar{h}^4)]\bar{h}^2\cos\theta, \tag{5.20}$$

$$\frac{\mathrm{Im}\,\omega}{\delta} = \frac{1}{\delta k}\left[\frac{1}{3}k^3\bar{h}^3 - \frac{3}{5}k^5\bar{h}^5 + O(k^7\bar{h}^7)\right](\lambda\sin\theta - \gamma k^2), \tag{5.21}$$

are not much better. For a better agreement, the film's thickness should be approximately 50 times smaller than the radius of the cylinder ($\delta = 0.02$) – see figure 4. But, in any case, the LA does *not* describe the maximum growth rate. Indeed, assume for simplicity that there is no surface tension ($\gamma = 0$) – then, the local growth rate (5.17) reaches its maximum at $k\bar{h} \approx 2$ (which can be deduced from figure 3*b*, where the maximum is located at $\bar{k}/\delta \approx 20$, with $\delta = 0.1$ and $\bar{h} = 1$). Thus, the wavelength (equal to $2\pi/k$) of the most unstable disturbance is, roughly, three times larger than the film's thickness and, thus, is inconsistent with the LA.

https://doi.org/10.1017/jfm.2013.530 Published online by Cambridge University Press

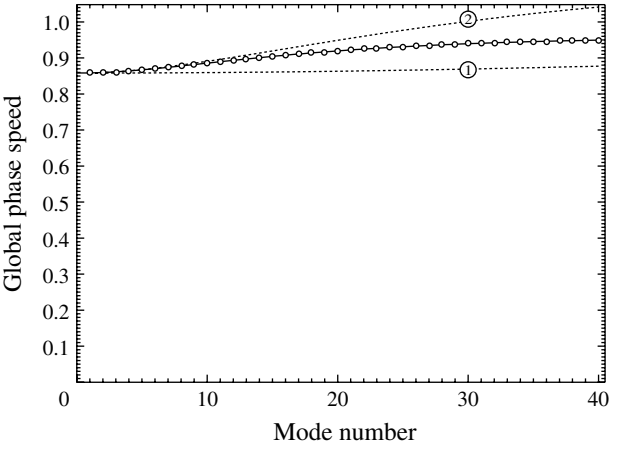

FIGURE 5. The 'global' phase speed $\omega/\delta n$ versus the mode number n, for $\delta = 0.02$, $\lambda = 0.35$, $\alpha = 0$ (Stokes flow), $\gamma = 0$ (no surface tension) and $l = 0$ (no axial variability). The corresponding LA solution is shown as the dotted lines: ①, the first-order solution; ②, the second-order solution.

5.3. *Examples of eigenmodes*

We shall now apply (5.15) to eigenmodes, in which case it determines the local azimuthal wavenumber m as a function of θ, for a given frequency ω and axial wavenumber l. Once $m(\theta)$ is computed, it should be substituted into the periodicity condition (5.4), which determines the dependence of ω on l and the mode number n.

This plan has been realized numerically, using the secant method for solving (5.15) for m, and Simpson's rule combined with the secant method for integrating and solving (5.4) for ω. For $\gamma = 0$ (no surface tension), only real (neutrally stable) eigenfrequencies were found, which agrees with the corresponding LA results obtained in the absence of inertial and capillary effects (Benjamin *et al.* 1993; Benilov *et al.* 2003). Typical results for $\gamma = 0$ are shown in figure 5, where we also compare the present approximation to the LA (as before, it holds when the film's thickness is 50 or more times smaller than the radius of the cylinder).

We have also examined the effect of surface tension in a wide range of γ and λ, and, in all cases, surface tension makes the disturbance decay ($\mathrm{Im}\,\omega < 0$). Thus, the capillary instability observed by O'Brien (2002) and Benilov *et al.* (2005) is an artefact of the LA (the possibility of which has indeed been pointed out in the latter paper).

5.4. *The existence of exploding solutions*

When studying the stability of rimming flows, Benilov *et al.* (2003), Benilov (2004) and Benilov *et al.* (2005) found exploding solutions that develop singularity in a finite time. These solutions, however, have been found using the LA, which becomes invalid when the spatial scale of the collapsing disturbances becomes comparable to the film's thickness (which might happen even before the breakdown of the linearity condition). In this section, we shall examine whether or not exploding solutions are admitted by the (more accurate) Stokes-flow approximation.

It is intuitively clear that exploding solutions can exist only if there is a spatial region where the local growth rate tends to plus infinity in the short-wave limit,

$$\mathrm{Im}\,\omega \to +\infty \quad \text{as } k \to \infty. \tag{5.22}$$

https://doi.org/10.1017/jfm.2013.530 Published online by Cambridge University Press

In the absence of surface tension ($\gamma = 0$), the leading-order LA growth rate (5.19) does satisfy this requirement (in the upper part of the cylinder), giving rise to the exploding solutions found in the above-mentioned papers. If $\gamma > 0$, expression (5.19) tends to *minus* infinity, in accordance with which no exploding solutions were found in the LA problem with surface tension (see Benilov *et al.* (2005) and Benilov (2006) for the azimuthal and axial disturbances, respectively).

In the present case, expression (5.17) for the local growth rate shows that

$$\mathrm{Im}\,\omega \to \begin{Bmatrix} 0 & \text{if } \gamma = 0 \\ -\infty & \text{if } \gamma > 0 \end{Bmatrix} \quad \text{as } k \to \infty. \tag{5.23}$$

Hence, the corresponding set of equations, (4.42)–(4.50), does not admit exploding solutions.

It should be emphasized, however, that the formal absence of singular solutions does not preclude disturbances from growth. It just transforms the *exploding* instability into a *transient* one (see Farrel 1982; Trefethen *et al.* 1993; Chapman 2002), such that the disturbance initially grows by an order of magnitude, but eventually always disperses. If, however, the transient growth is strong enough to trigger off nonlinear effects, the steady state breaks down *before* the dispersal of the linear disturbance.

The above argument agrees with the conclusions of Benilov (2006) obtained for a similar problem, where surface tension was indeed shown to transform exploding disturbances into transient ones.

6. Inertial instability of rimming flows

In this section, we shall examine the general case, $\alpha \neq 0$, where instability is expected to occur due to the effects of inertia (described by the material derivatives of the Navier–Stokes equations). Benilov & O'Brien (2005) examined this type of instability using the LA and demonstrated that its growth rate grows monotonically with the mode number – hence, the maximum growth occurs at *short* wavelengths. Thus, the LA (which is inapplicable to short disturbances) is not suitable for studying inertial instability, whereas the WKB method used earlier in this paper is.

Substituting the WKB representation (5.3) and (5.5) into the first three of the Navier–Stokes equations, (4.46)–(4.48), keeping the leading-order terms only, and omitting hats and superscripts, we obtain

$$\mathrm{i}\alpha(m\bar{v} - \omega)U + \frac{\partial P}{\partial r} = \frac{\partial^2 U}{\partial r^2} - k^2 U, \quad \mathrm{i}\alpha(m\bar{v} - \omega)V + \mathrm{i}mP = \frac{\partial^2 V}{\partial r^2} - k^2 V, \tag{6.1}$$

$$\mathrm{i}\alpha\left[(mV - \omega)W + U\frac{\partial \bar{v}}{\partial r}\right] + \mathrm{i}lP = \frac{\partial^2 W}{\partial r^2} - k^2 W, \tag{6.2}$$

where the effective Reynolds number α is given by (3.2), and $k^2 = m^2 + l^2$. The remaining equations are exactly the same as in the Stokes-flow limit, i.e. coincide with (5.9)–(5.13).

Unlike the Stokes-flow limit, the coefficients of the problem for $\alpha \neq 0$ involve r and, therefore, the dependence of the eigenmode on r cannot be resolved analytically. Instead, it was resolved numerically, using the Runge–Kutta method. The rest of the scheme remains the same as in § 5.3.

https://doi.org/10.1017/jfm.2013.530 Published online by Cambridge University Press

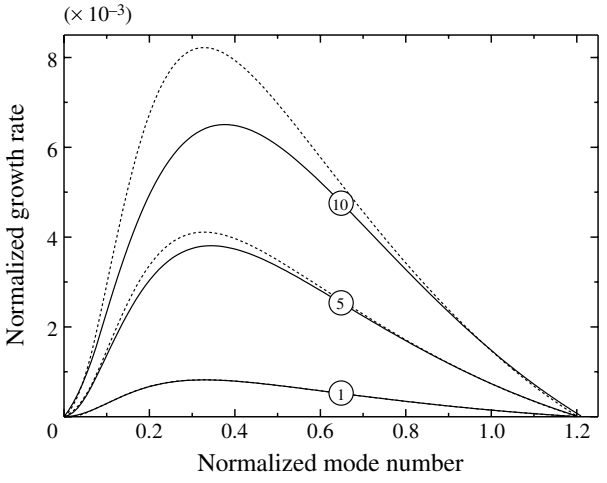

FIGURE 6. The normalized growth rate $\mathrm{Im}\,\omega$ of inertial instability versus the normalized mode number $N = n\delta$, for $\lambda = 0.35$, $\alpha = 1,\ 5,\ 10$, $\gamma = 0$ (no surface tension) and $l = 0$ (no axial variability). The curves are marked with the corresponding values of α. The dotted curves were computed for $\alpha = 0.1$ and scaled up by the factors of 10, 50 and 100 (the first of the three curves is indistinguishable from the case $\alpha = 1$).

6.1. *The results*

The eigenvalue problem (6.1), (6.2), (5.9)–(5.13) and (5.4) has been solved for a wide range of the parameters involved, with typical results shown in figures 6–8. Note that these figures have been drawn in terms of the *normalized* growth rate $\mathrm{Im}\,\omega$ and the *normalized* mode number $N = n\delta$ (as opposed to the actual rate $\mathrm{Im}\,\omega/\delta$ and the actual mode number n, defined by (4.42)–(4.44) and (5.4) and used in figure 5). The normalized variables make the graph continuous and independent of δ, whereas the eigenmodes correspond to N being exact multiples of δ.

The following conclusions have been drawn.

(*a*) As the axial wavenumber l increases, the growth rate of inertial instability always decays. Thus, the strongest instability occurs for $l = 0$, i.e. for two-dimensional disturbances.

(*b*) It turned out that, even for large values of α, the normalized growth rate $\mathrm{Im}\,\omega$ is anomalously small (see figure 7). This came as a surprise, as $\mathrm{Im}\,\omega$ does not depend on any small or large parameter.

(*c*) Furthermore, for $\alpha \lesssim 5$, the growth rate is almost proportional to α. To illustrate this, we computed $\mathrm{Im}\,\omega$ for $\alpha = 0.1$, multiplied it by 10, 50 and 100, and compared with $\mathrm{Im}\,\omega$ computed for $\alpha = 1,\ 5,\ 10$ (see figure 7). Observe that, even for $\alpha = 10$, the two graphs are not too far apart.

This suggests that an asymptotic theory for small Reynolds numbers ($\alpha \to 0$) would be accurate for at least $\alpha \lesssim 5$.

(*d*) With increasing λ, inertial instability becomes stronger (see figure 8) – i.e. thick films are more unstable than thin ones.

(*e*) Surface tension weakens instability, especially higher eigenmodes (see figure 9). A similar tendency has been observed in the LA analysis of Benilov & O'Brien

https://doi.org/10.1017/jfm.2013.530 Published online by Cambridge University Press

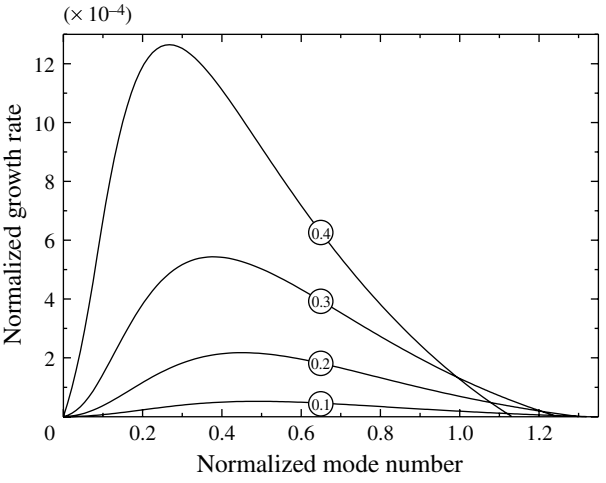

FIGURE 7. The same as figure 6, but for $\lambda = 0.1,\ 0.2,\ 0.3,\ 0.4$, $\alpha = 1$ and $\gamma = 0$ (no surface tension). The curves are marked with the corresponding values of λ.

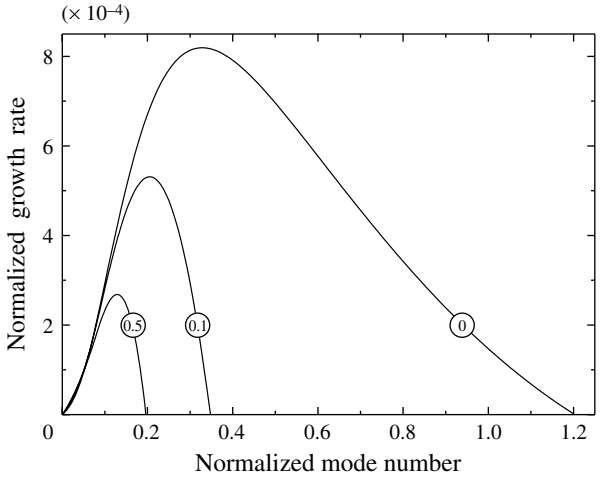

FIGURE 8. The same as figures 6 and 7, but for $\lambda = 0.35$, $\alpha = 1$ and $\gamma = 0,\ 0.1,\ 0.5$. The curves are marked with the corresponding values of γ.

(2005). Thus, the last eigenmode to remain unstable is the first one, $n = 1$ (to which the latter work is applicable).

Thus, if one needs to find out whether or not a given rimming flow is stable, one should be able to rely on the first-mode LA. Then, if the flow is *unstable*, the growth rate can be calculated either through the LA (for marginally unstable flows), or through the WKB theory presented here (for cases where instability is strong enough to reach high eigenmodes).

Note, however, that the above argument implies that the WKB approximation and LA 'overlap', so the wavelength of maximum growth is described by at least one of the two. To verify that this is indeed the case, note that the WKB applies

https://doi.org/10.1017/jfm.2013.530 Published online by Cambridge University Press

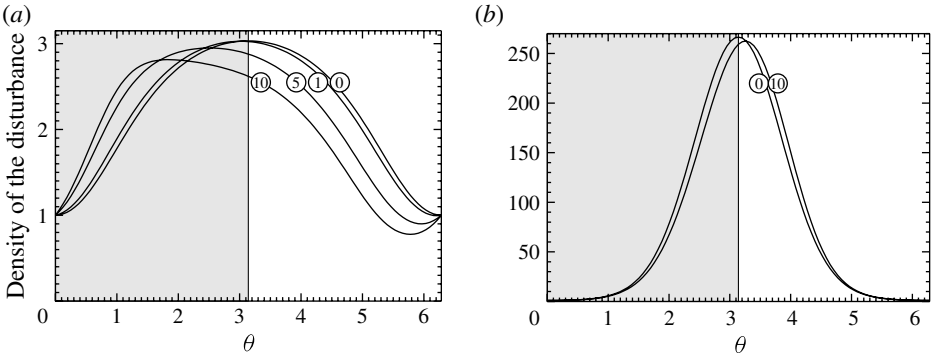

FIGURE 9. The density of the disturbance (defined by (6.5)) versus θ for $\lambda = 0.35$, $\alpha = 0,\ 1,\ 5,\ 10$, $\gamma = 0$ and $l = 0$ for: (*a*) an unstable eigenmode, $n = 15$; and (*b*) a stable eigenmode, $n = 80$. The curves are marked with the corresponding values of α. The region of local instability (the cylinder's upper half) is shaded.

to (dimensional) wavelengths that are much shorter than the cylinder's radius R – whereas the LA applies to wavelengths longer than the characteristic depth $\langle h \rangle$ of the liquid. Thus, the two approximations are both applicable to wavelengths longer than $\langle h \rangle$, but shorter than R.

(*f*) Note, however, that surface tension can stop inertial instability only for very small cylinders. Even the flow in example (3.12)–(3.13), where $R = 3$ cm, is noticeably unstable, with the e-folding time being approximately 15 s. To stabilize it (keeping the same value of $\delta = \langle h \rangle / R$), one needs to reduce the cylinder's radius to $R \lesssim 0.75$ cm (this estimate has been obtained using the approach of Benilov & O'Brien (2005)).

Thus, reducing the Reynolds number (through increasing the fluid's viscosity or reducing the cylinder's angular velocity) seems to be the only way to inhibit inertial instability (which is essential for industrial applications).

6.2. *Discussion: the mechanism of inertial instability*

Recall that, for $\alpha = \gamma = 0$ (i.e. for a Stokes flow with no surface tension), the local growth rate (5.17) is positive (unstable) in the upper part of the cylinder and negative (stable) in the lower part. Observe also that the governing equations (5.6)–(5.12) are invariant with respect to the simultaneous replacements

$$\theta \to -\theta, \quad U, P \to U^*, P^*, \quad V, W, H \to -V^*, -W^*, -H^*, \quad \omega \to \omega^*. \tag{6.3}$$

Accordingly, the eigenfunctions are symmetric with respect to the point $\theta = \pi$,

$$|U(-\theta, r)| = |U(\theta, r)|, \quad |V(-\theta, r)| = |V(-\theta, r)|, \quad \ldots, \tag{6.4}$$

and the disturbances are neutrally stable, as they are 'equipartitioned' between the cylinder's stable and unstable halves.

If, however, $\alpha \neq 0$, the governing equations (6.1)–(6.2) are *not* invariant with respect to (6.3). The eigenfunctions are no longer symmetric and the disturbances are not equipartitioned between the upper and lower parts of the cylinder – hence, they become either asymptotically stable or fully unstable.

https://doi.org/10.1017/jfm.2013.530 Published online by Cambridge University Press

To illustrate the above observation, introduce

$$D(\theta) = \left| \exp\left[\frac{\mathrm{i}}{\delta} \int_0^\theta m(\theta')\, \mathrm{d}\theta' \right] \right|, \tag{6.5}$$

which will be referred to as the *density of the disturbance* (it appears in the WKB representations of all the unknowns – see (5.3)). Several examples of $D(\theta)$ are shown in figure 9. One can see that, if $\alpha = 0$, the density of the disturbance is indeed symmetric and, thus, corresponds to neutral stability. For positive α, on the other hand, the graph of $D(\theta)$ becomes increasingly 'skewed' towards the cylinder's *upper* half, as the disturbance becomes more and more *unstable* (see figure 9*a*). Note also that, for *stable* disturbances, $D(\theta)$ is skewed towards the cylinder's *lower* half, although by a much smaller margin (see figure 9*b*).

We conclude that inertial effects violate the symmetry of disturbances and 'skew' some of them towards the cylinder's upper half, making them unstable.

7. Summary and concluding remarks

Thus, we have examined the stability of rimming flows. Five non-dimensional parameters, (3.1)–(3.5), have been introduced, in terms of which requirements (3.6)–(3.10) of the LA were formulated. Then, assuming that the steady flow satisfies all of these requirements, we allowed the disturbance's wavelength to be comparable to the film's thickness (and, thus, to violate some of the LA requirements, namely (3.7), (3.9) and (3.11)). For harmonic disturbances (eigenmodes), a linearized set of equations, (4.46)–(4.54), has been derived and then solved by a WKB-style asymptotic method based on a 'locally harmonic' dependence of the eigenfunction on the azimuthal coordinate (see (5.3)).

Firstly, we examined the limit of small Reynolds number ($\alpha \to 0$, where α is defined by (3.2)), in which case the equations for the disturbance reduce to the Stokes-flow approximation. The following conclusions have been drawn.

(*a*) In the absence of surface tension, the disturbance grows in the upper part of the cylinder and decays in the lower part. The maximum growth occurs for the disturbance, the wavelength of which is approximately three times larger than the film's thickness. Such disturbances do *not* satisfy the LA.

(*b*) Despite the local instability, the 'global' harmonic solutions (eigenmodes) are neutrally stable, which reflects the perfect balance between the disturbance's growth in the upper part of the cylinder and its decay in the lower part. A similar property has been pointed out by Benjamin *et al.* (1993) and Benilov *et al.* (2003) for the long-wave eigenmodes (tractable through the LA).

Secondly, we considered the general case, $\alpha \neq 0$, which takes into account inertial effects. The following conclusions have been drawn.

(*a*) It was shown that inertia violates the balance between the cylinder's upper and lower halves. As a result, some of the eigenmodes become 'skewed' towards the former and, thus, become unstable.

(*b*) As the axial wavenumber increases, the growth rate of inertial instability decays. Thus, the strongest instability occurs for two-dimensional disturbances.

(*c*) Surface tension weakens slightly inertial instability and, in principle, can eliminate it – but the complete stabilization occurs only for very small cylinders, with a radius of less than 1 cm.

https://doi.org/10.1017/jfm.2013.530 Published online by Cambridge University Press

Finally, we shall discuss the implications of our results for the original problem of honey on a rotating spoon (Moffatt 1977). Even though a quantitative prediction cannot be made (as cylinders are not good approximations of spoons), one can still conjecture that surface tension can stabilize flows on smaller (tea)spoons. For larger ones, however, a thin layer of honey (such that Moffatt's (1977) smooth solution applies) is likely to be unstable.

A thick layer, on the other hand – such that a shock solution applies – can actually be stable even on a large spoon. Such flows have not been considered in this paper, but Benjamin *et al.* (1993) and O'Brien & Gath (1998) argued that they are stable due to absorption of potentially unstable perturbation in the shock, similar to those in gas shocks and tidal bores. This conclusion agrees with the numerical results of Peterson, Jimack & Kelmanson (2001), who observed increasing stability in the limit $\lambda \to 4/9$, i.e. when the steady state approached the parameter region of shock-wave solutions.

Note, however, that the analyses of Benjamin *et al.* (1993) and O'Brien & Gath (1998) have been carried out using the lubrication approximation (LA) – which, firstly, neglects inertial instability and, secondly, is invalid near the shock. As a result, conclusions obtained through the LA can be incorrect both quantitatively and qualitatively (regarding the latter, see Benilov & Lapin (2011) and Benilov *et al.* (2012)).

In a more accurate non-LA model, the stability of shock solutions results from a competition between the inertial instability and the absorption of unstable disturbances in the shock, so that some of the flows are stable and some are not. The cases for which the two effects are in precise balance determine both the maximum and minimum amounts of honey that can be kept on a rotating spoon.

Acknowledgement

The authors acknowledge the support of the Science Foundation Ireland under grants 11/RFP.1/MTH3281 and 12/IA/1683.

Appendix. Solution of the boundary-value problem (5.6)–(5.13)

Consider the following combination of (5.6)–(5.8):

$$\frac{\partial}{\partial r}(5.6) + \mathrm{i}m(5.7) + \mathrm{i}l(5.8), \tag{A 1}$$

which yields

$$\frac{\partial^2 P}{\partial r^2} - k^2 P = 0. \tag{A 2}$$

The solution of this equation can be written in the form

$$P = c_1 \cosh kr + c_2 \sinh kr, \tag{A 3}$$

where the 'constants' of integration $c_{1,2}$ may depend on θ. Substituting (A 3) into (5.6)–(5.8), solving for U, V, W, and taking into account boundary conditions (5.10), we obtain

$$U = \frac{1}{2}[c_1 r \cosh kr + (c_4 + c_2 r)\sinh kr], \tag{A 4}$$

$$V = \frac{\mathrm{i}m}{2k}[(c_5 + c_1 r)\sinh kr + c_2 r \cosh kr], \tag{A 5}$$

$$W = \frac{\mathrm{i}l}{2k}[(c_7 + c_1 r)\sinh kr + c_2 r \cosh kr]. \tag{A 6}$$

https://doi.org/10.1017/jfm.2013.530 Published online by Cambridge University Press

Substitution of (A 4)–(A 6) into the continuity equation (5.9) yields

$$c_4 = -\frac{c_1}{k}, \quad c_2 = \frac{m^2 c_5 + l^2 c_7}{k}. \tag{A 7}$$

Using (A 7) to eliminate c_4 and c_2 from (A 4)–(A 6) and (A 3), and substituting the resulting expressions for U, V, W and P into the free-surface boundary conditions (5.12) and (5.13) gives

$$(k\bar{h}\sinh k\bar{h} - \cosh k\bar{h})c_1 + (m^2\bar{h}\cosh k\bar{h})c_5 + (l^2\bar{h}\cosh k\bar{h})c_7 = H(\sin\theta - \gamma k^2), \tag{A 8}$$

$$(2k^2\bar{h}\cosh k\bar{h})c_1 + [2m^2 k\bar{h}\sinh k\bar{h} + (k^2+m^2)\cosh k\bar{h}]c_5 + [l^2(2k\bar{h}\sinh k\bar{h} + \cosh k\bar{h})]c_7 = \frac{2\mathrm{i}k^2 H\cos\theta}{m}, \tag{A 9}$$

$$(2k^2\bar{h}\cosh k\bar{h})c_1 + [m^2(2k\bar{h}\sinh k\bar{h} + \cosh k\bar{h})]c_5 + [2l^2 k\bar{h}\sinh k\bar{h} + (k^2+l^2)\cosh k\bar{h}]c_7 = 0. \tag{A 10}$$

Using these equations, we can relate c_1, c_5 and c_7 to H,

$$c_1 = -\frac{(2k\bar{h}\sinh k\bar{h} + \cosh k\bar{h})(\sin\theta - \gamma k^2) - 2\mathrm{i}m\bar{h}(\cosh k\bar{h})\cos\theta}{2(\cosh^2 k\bar{h} + k^2\bar{h}^2)}H, \tag{A 11}$$

$$c_5 = \frac{(\bar{h}\cosh^2 k\bar{h})(\sin\theta - \gamma k^2)}{[\cosh^2 k\bar{h} + (k\bar{h})^2]\cosh k\bar{h}}H - \frac{\mathrm{i}[m^2 k\bar{h}(\cosh k\bar{h})(\sinh k\bar{h}) - (k^2+l^2)\cosh^2 k\bar{h} - 2l^2(k\bar{h})^2]\cos\theta}{mk^2[\cosh^2 k\bar{h} + (k\bar{h})^2]\cosh k\bar{h}}H, \tag{A 12}$$

$$c_7 = \frac{(\bar{h}\cosh^2 k\bar{h})(\sin\theta - \gamma k^2)}{[\cosh^2 k\bar{h} + (k\bar{h})^2]\cosh k\bar{h}}H - \frac{\mathrm{i}m[k\bar{h}(\cosh k\bar{h})(\sinh k\bar{h}) + \cosh^2 k\bar{h} + 2(k\bar{h})^2]\cos\theta}{k^2[\cosh^2 k\bar{h} + (k\bar{h})^2]\cosh k\bar{h}}H. \tag{A 13}$$

Now, substitute expression (A 4) for U into (5.11) and take into account (A 7)–(A 13), after which H cancels out, and we end up with (5.15).

Observe also that the cancellation of H prevents us from finding the solution for U, V, W and P. This is typical of the WKB approach, where the leading-order solution yields the 'eikonal' (i.e. $m(\theta)$), but not the amplitude of the eigenfunction. To determine the latter, one needs to examine the next order, as has been done by Benilov *et al.* (2003) for the LA version of the present problem.

Note, however, that there is no point in doing so for our equations (5.6)–(5.13), as they include only the *leading* order of the linearized Navier–Stokes set – whereas, to consistently determine $H(\theta)$, the *next-to-leading* order should be taken into account. Alternatively, we have to confine ourselves to the eigenfrequency ω, which is the most important stability characteristic anyway.

In the present paper, we choose the latter option, as the former one results in extremely cumbersome algebra. Furthermore, even though the next-order expansion fixes $H(\theta)$, it is unlikely to improve on the leading-order eigenfrequency (in all the WKB techniques known to the authors, the eigenvalue expansions skip every other term).

https://doi.org/10.1017/jfm.2013.530 Published online by Cambridge University Press

REFERENCES

ASHMORE, J., HOSOI, A. E. & STONE, H. A. 2003 The effect of surface tension on rimming flows in a partially filled rotating cylinder. *J. Fluid Mech.* **479**, 65–98.

BENILOV, E. S. 2004 Explosive instability in a linear system with neutrally stable eigenmodes. Part 2: Multi-dimensional disturbances. *J. Fluid Mech.* **501**, 105–124.

BENILOV, E. S. 2006 Does surface tension stabilize a liquid film inside a rotating horizontal cylinder? Part 2: Multi-dimensional disturbances. *Stud. Appl. Maths* **116**, 1–20.

BENILOV, E. S., BENILOV, M. S. & KOPTEVA, N. 2008 Steady rimming flows with surface tension. *J. Fluid Mech.* **597**, 91–118.

BENILOV, E. S., KOPTEVA, N. & O'BRIEN, S. B. G. 2005 Does surface tension stabilize a liquid film inside a rotating horizontal cylinder? *Q. J. Mech. Appl. Maths* **58**, 158–200.

BENILOV, E. S., LACEY, S. M. & O'BRIEN, S. B. G. 2005 Exploding solutions for three-dimensional rimming flows. *Q. J. Mech. Appl. Maths* **58**, 563–576.

BENILOV, E. S. & LAPIN, V. N. 2011 Shock waves in Stokes flows down an inclined plate. *Phys. Rev.* E **83**, 066321.

BENILOV, E. S., LAPIN, V. N. & O'BRIEN, S. B. G. 2012 On rimming flows with shocks. *J. Engng Maths* **75**, 49–62.

BENILOV, E. S. & O'BRIEN, S. B. G. 2005 Inertial instability of a liquid film inside a rotating horizontal cylinder. *Phys. Fluids* **17**, 052106.

BENILOV, E. S., O'BRIEN, S. B. G. & SAZONOV, I. A. 2003 A new type of instability: explosive disturbances in a liquid film inside a rotating horizontal cylinder. *J. Fluid Mech.* **497**, 201–224.

BENJAMIN, T. B., PRITCHARD, W. G. & TAVENER, S. J. 1993 Steady and unsteady flows of a highly viscous liquid inside a rotating horizontal cylinder (unpublished manuscript).

CHAPMAN, S. J. 2002 Subcritical transition in channel flow. *J. Fluid Mech.* **451**, 35–97.

FARREL, B. F. 1982 Modal and nonmodal baroclinic waves. *J. Atmos. Sci.* **41**, 1663–1686.

FINN, R. 1986 *Equilibrium Capillary Surfaces*. Springer.

LANDAU, L. & LIFSHITZ, E. 1995 *Course of Theoretical Physics, vol. 6, Fluid Mechanics*. Pergamon.

LESLIE, G. A., WILSON, S. K. & DUFFY, B. R. 2013 Three-dimensional coating and rimming flow: a ring of fluid on a rotating horizontal cylinder. *J. Fluid Mech.* **716**, 51–82.

MOFFATT, H. K. 1977 Behaviour of a viscous film on the outer surface of a rotating cylinder. *J. Méc.* **16**, 651–574.

O'BRIEN, S. B. G. 1998 A model for the coating of cylindrical light bulbs. In *Progress in Industrial Mathematics* (ed. L. Arkeryd, J. Bergh, P. Brenner & R. Pettersson), pp. 46–55. B. G. Teubner.

O'BRIEN, S. B. G. 2002 A mechanism for two dimensional instabilities in rimming flow. *Q. Appl. Maths* **60**, 283–300.

O'BRIEN, S. B. G. & GATH, E. G. 1998 The location of a shock in rimming flow. *Phys. Fluids* **10**, 1040–1042.

PETERSON, R. C., JIMACK, P. K. & KELMANSON, M. A. 2001 On the stability of viscous free-surface flow supported by a rotating cylinder. *Proc. R. Soc. Lond.* A **457**, 1427–1445.

POUGATCH, K. & FRIGAARD, I. 2011 Thin film flow on the inside surface of a horizontally rotating cylinder: steady state solutions and their stability. *Phys. Fluids* **23**, 022102.

THRONE, J. L. & GIANCHANDANI, J. 1980 Reactive rotational molding. *Polym. Engng Sci.* **20**, 899–919.

TREFETHEN, L. N., TREFETHEN, A. E., REDDY, S. C. & DRISCOLL, T. A. 1993 Hydrodynamic stability without eigenvalues. *Science* **261**, 578–584.

WILLIAMS, J., HIBBERD, S., POWER, H. & RILEY, D. S. 2012 On the effects of mass and momentum transfer from droplets impacting on steady two-dimensional rimming flow in a horizontal cylinder. *Phys. Fluids* **24**, 053103.

WILSON, S. K., HUNT, R. & DUFFY, B. R. 2002 On the critical solutions in coating and rimming flow on a uniformly rotating horizontal cylinder. *Q. J. Mech. Appl. Maths* **55**, 357–383.

https://doi.org/10.1017/jfm.2013.530 Published online by Cambridge University Press